

# Multidisciplinary design optimization of an accumulator for a large elasticity range of flexible webs

Dominique Knittel<sup>1,2,a</sup>, David Kuhm<sup>1,3</sup>, Jean Renaud<sup>2</sup>

<sup>1</sup>Centre d'Innovation et de Transfert Technologique (CITT), University of Strasbourg, 17 rue du Maréchal Lefebvre, 67100 Strasbourg

<sup>2</sup>Laboratoire de Génie de la Conception INSA Strasbourg, 24 boulevard de la Victoire, 67084 Strasbourg, France

<sup>3</sup>Laboratoire de Laboratoire de Physique et Mécanique Textiles, ENSISA, 11 rue Alfred Werner, 68093 Mulhouse, France

Received 20 September 2010, Accepted 22 November 2010

**Abstract**—This paper concerns the optimization of an accumulator used in an industrial elastic web processing plant (paper, fabric, polymer, metal ...). A nonlinear model of an industrial accumulator is first detailed which enables to deduce a linear model. These models are derived from the physical laws describing web tension and velocity dynamics in each web span. The effects of time-varying rheological and mechanical parameters, such as web Young modulus, web length and rolls inertia, on accumulator dynamics and performances are analyzed. The second part presents several optimizations of industrial PI controllers using evolutionary algorithm for a realistic non-linear model, in conjunction with the controllers interpolation strategy. Finally, simulations made in the Matlab/Simulink software environment show performances improvements compared to hand tuned controllers.

**Keywords:** Industrial accumulator, Roll-to-roll, Dynamic modeling, PI controller optimization, Mono-objective optimization

## 1 Introduction

In many plants, accumulators (Fig. 1) are used to allow for rewind or unwind core change while the process continues at a constant velocity. Such systems store web during the regular phase of production. The web is then released during the wound roll change, in the case of an entry accumulator. Using an accumulator allows nonstop operation on the production line.

During the regular production phase, the accumulator carriage is placed at its nominal position. When the unwinder wound roll is almost empty, the accumulator carriage is moved up (vertically in our studied processing line) in order to maximize the web storage into the accumulator. However, during the unwinder roll change, the accumulator carriage is adequately moved down in order to release the web for having a constant web velocity. Finally, after the roll change, the accumulator carriage is moved to its initial position. The unwinder roll changing time will take place in very short time depending on the accumulated web length.

The web tensions inside the accumulator are easy to control in standard operating conditions (when the accumulator carriage is placed at its constant nominal position). Nevertheless, web tensions variations can often appear during the transition phases and generate web folds or breaks due to the inertia and friction of many free rollers.

Different works in web tension control of roll-to-roll systems have been published during the last years. For example Zalhan et al. [23], Brandenburg [2], Benlatreche et al. [1], Knittel et al. [6] [8], Gassmann et al. [4] present the modeling and control of a continuous processing line composed only with tractors and free rollers, whereas Wolfermann [22], Gassmann [18], Knittel et al. [7] describe the unwinding and winding process. Only few papers present the modeling and control of industrial accumulators. Important results can be

found in Koç et al. [11] [12], Pagilla et al. [19] [20], Kuhm et al. [13] [14] and Knittel et al. [15].

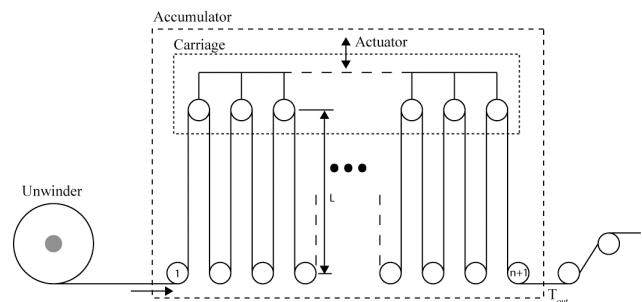


Fig. 1. Sketch of an industrial accumulator

In the second part of this paper, the accumulator model based on physical laws is described. This part also highlights the effect of mechanical parameters variations on the accumulator dynamic performances. The third part presents different accumulator optimization strategies. First, a mono-objective PI controller optimization is made. Then, controllers are optimized in conjunction with an interpolation strategy. The last PI controller optimization strategy, taking into account Young modulus variation, is performed. Finally simulation results obtained in the Matlab/Simulink software environment with a realistic accumulator model are presented.

## 2 Plant modeling

### 2.1 Nonlinear model of the accumulator

#### Web tension calculation:

Assuming there is no sliding between web and rollers, the equation of continuity applied to the web span between two consecutive rollers (Fig. 2) gives (Koç [9], Koç et al. [10]) :

$$\frac{d}{dt} \left( \frac{L_k}{1 + \varepsilon_k} \right) = -\frac{V_{k+1}}{1 + \varepsilon_k} + \frac{V_k}{1 + \varepsilon_{k-1}} \quad (1)$$

where  $L_k$  is the variable web length between the  $k^{\text{th}}$  and the  $(k+1)^{\text{th}}$  rollers. This length can vary due to the accumulator carriage motion.  $V_k$  is the linear velocity of the  $k^{\text{th}}$  roll and  $\varepsilon_k$  represents the strain of the  $k^{\text{th}}$  web span. Web tension  $T_k$  is then deduced from relation (1) by applying the Hooke's law (see Koç [9] or Koç et al. [10]).

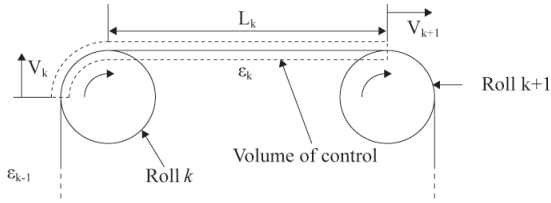


Fig. 2. Indices of web span between two consecutive rollers

### Web velocity calculation:

The velocity dynamic of the  $k^{\text{th}}$  roll is calculated by using the torque balance. Assuming there is no slippage between the web and the roll, the web velocity  $V_k$  is equal to the linear velocity of the roll. This velocity dynamic is given by equation 2:

$$\frac{d}{dt} (J_k \cdot \Omega_k) = C_{mk} - C_{rk} - C_{fk} \quad (2)$$

Where  $\Omega_k = V_k / R_k$  is the angular velocity of the  $k^{\text{th}}$  roll,  $J_k$  the roll inertia and  $R_k$  the roll radius.  $C_{mk}$  is the motor torque for a driven roll.  $C_{rk}$  and  $C_{fk}$  stand for the resistive torque introduced by the web and friction torque between the roll and its shaft respectively. The equations (1) and (2) are applied to each web span and roll of the studied accumulator and enable the construction of a non-linear longitudinal web dynamics simulator.

### Accumulator representation:

The inputs/outputs block scheme of the studied accumulator is shown in Fig. 3. The system has three inputs:  $V_{in\,accu}$  which is the web speed at the entrance of the accumulator,  $V_{out\,accu}$  the web speed at the exit and  $L$  that is the time-varying length between two consecutive rollers (depending on accumulator carriage position). The system output is the web span tension  $T_{out}$  just after the last roll in the accumulator, (see Fig. 1).

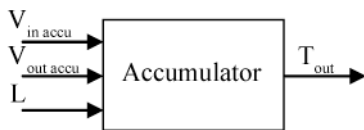


Fig. 3. Input / Output scheme of the accumulator

### Accumulator carriage velocity reference:

In the phase of wound roll change, the accumulator output speed  $V_{out\,accu}$  is maintained at the nominal speed  $V_{ref}$  whereas the input speed  $V_{in\,accu}$  decreases to zero. In

order to maintain the output web tension and speed constant during this change, it is necessary to move adequately the accumulator carriage. In our study, the accumulator is composed of  $n+1$  rollers and therefore has  $n$  web spans. The accumulator carriage displacement speed reference is given by the following relation:

$$V_{accu} = \frac{1}{n} (V_{in\,accu} - V_{out\,accu}) \quad (3)$$

### Unwinder speed reference during accumulation phase:

During the web storing phase, the unwinder speed reference has to be increased. This unwinding speed can be deduced from the equation (3):

$$V_{in\,accu} = nV_{accu} + V_{out\,accu} \quad (4)$$

## 2.2 Linear model of the accumulator

### Linearization:

The linear model can be deduced from the nonlinear one around a working point. The web span dynamic linearization are detailed in Koç [9] and Kuhm et al. [13].

### State space representation:

The linear model of the accumulator can be described by a state space representation given in (5). This linear model is useful for Bode diagrams calculation.

$$\begin{cases} \dot{x} = \left( A + \frac{A1}{L} \right) x + \frac{B}{L} u + B1 v \\ Y = Cx + Du \end{cases} \quad (5)$$

where

$$x = \begin{bmatrix} T_{in} \\ V_1 \\ T_1 \\ \vdots \\ V_{n+1} \\ T_{n+1} \end{bmatrix} \quad u = \frac{dL}{dt} \quad v = \begin{bmatrix} V_{in\,accu} \\ V_{out\,accu} \end{bmatrix}$$

### Influence of the mechanical parameters

Two transfer functions have been studied in our accumulator (Fig. 3): one between the accumulator output tension  $T_{out}$  and the accumulator input velocity  $V_{in\,accu}$  named  $W_1$  and the other between  $T_{out}$  and the web span length  $L$  named  $W_2$ . In industrial accumulators, mainly two control strategies are applied: one using  $V_{in\,accu}$  as control signal (controller output), the other using  $L$ . In this paper, we use a combination of the two strategies. In the following parts, the influences of some physical parameter variations around their nominal values are analysed on simulated Bode diagrams.

### Influence of the elasticity modulus:

The web elasticity influences the web dynamics (tension and velocity) in the transient phases. One can observe on Fig. 4 that the static gain and the resonances (gains and frequencies) are depending on the web Young modulus. Similar observations have been made for transfer functions  $W_1$ . Very often in the industry, Young modulus changes occur during the manufacturing process and therefore the control performances are decreasing if the controllers synthesis do not take into account the web elasticity variations. Consequently, the

controllers have to be adjusted for each range of web elasticity, or robust for a given (large) web elasticity range.

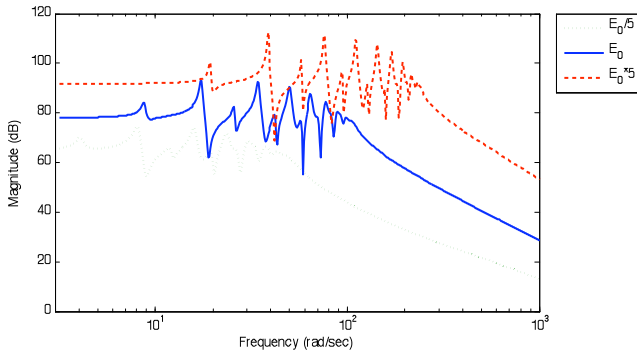


Fig. 4. Bode diagram of  $W_2$  for different Young modulus

**Variations of web span length:**

Like the Young modulus, the web span length in the accumulator (related to the position of the carriage) has a significant influence on the web dynamic (Fig. 5).

A long web span will have a weaker resonance frequency and a lower gain. This observation has been made for both transfer functions  $W_1$  and  $W_2$ . Therefore the dynamic sensitivity to the web length variations has to be taken into account in the controller synthesis because the web span length is varying each time a wound roll change occurs.

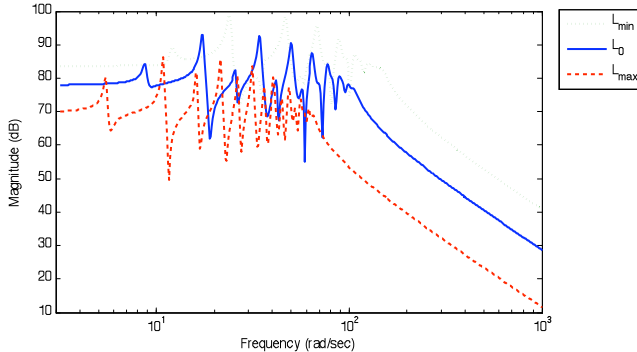


Fig. 5. Bode diagram of  $W_2$  for different web span lengths

**Study of the influence of roll inertia:**

The free rollers inertia also influences the web dynamics. As we can observe on Fig. 6, these inertias should be as weak as possible. Indeed important inertias strongly decrease the bandwidth of the system; this low bandwidth will make it difficult to control the accumulator. On the contrary, the inertia has no effect on the static gain. This has been observed for both transfer functions  $W_1$  and  $W_2$ .

**Influence of other parameters**

The shaft/roll frictions have low effect on the system bandwidth. A change of the friction value during the production will thus have a minor influence on the controller performances.

The nominal web velocity doesn't influence the system bandwidth. But a high speed reduces the resonance peaks. This effect doesn't depend on the web span length.

The nominal tension doesn't have any effect on the accumulator bandwidth and on the resonance peaks. This has been observed for both transfer functions  $W_1$  and  $W_2$ . More detailed analysis can be found in Kuhm *et al.* [13].

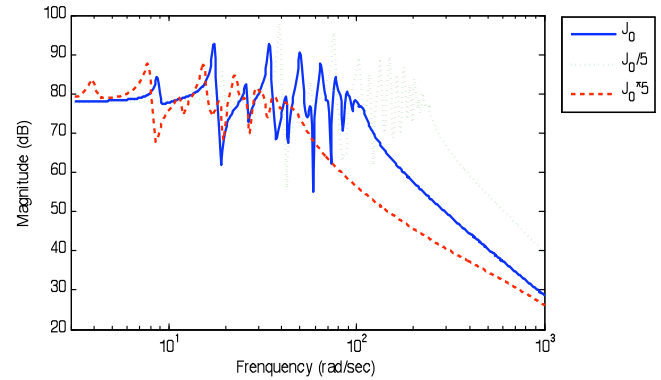


Fig. 6. Bode diagram of  $W_2$  for different roll inertia

**Remarks**

This previous part shows that the most influent parameters in our studied industrial accumulator are the web Young modulus (which describes the web elasticity), the rollers inertias and the web span length.

**3 Accumulator optimization**

**3.1 Accumulator control scheme**

As indicated in the precedent part, the accumulator has two different entries used as control signals.

An output web tension controller can be synthesized by using the input velocity of the accumulator as control signal. The second control strategy needs the web length (by moving the accumulator carriage) as control signal. In industrial applications, both control schemes are programmed. This study combines the two strategies. During the regular production phase, we use the input velocity as actuator and during the wound roll change we use the web length as actuator. The switching strategy between the two controllers is performed by weighting the controllers output by a coefficient  $\beta$  varying between 0 and 1. The control scheme is illustrated on Fig. 7.

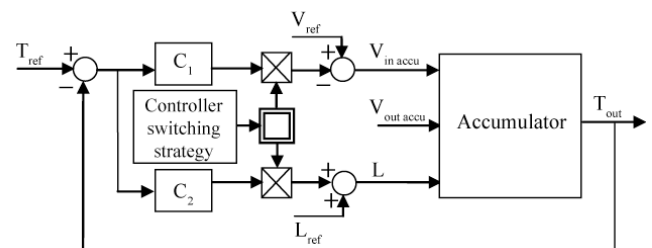


Fig. 7. Control scheme

These two PI controllers  $C_1$  and  $C_2$  have the following form:

$$C_i(s) = K_i \frac{1 + \tau_i s}{s} \quad (6)$$

### 3.2 Optimization strategies

#### Mono-objective controllers optimization

The PI parameters  $K_1$  and  $\tau_1$  for the first and  $K_2$  and  $\tau_2$  for the second controller are determined with an optimization approach for our realistic non-linear model. Controller optimization approaches are presented for example in Frechard et al. [3], Lin et al. [17], Popov et al. [21] and Zielinski et al. [24]. Robust controller optimization can be found in Gassmann et al [5], Knittel et al. [16] and Kuhm et al. [14].

The PI parameters are optimized using an evolutionary algorithm minimizing a first cost function  $J$  given in (7). In this cost function, the parameter  $\alpha$  is fixed at 10 in order to better minimize the tension peaks [15]. Another approach is to use the ITAE criterion as a cost function (see (8)). Using the ITAE criterion allows to minimize the static error.

$$J = \alpha \int_0^{t_{max}} (T_{out} - T_{ref})^\alpha dt \quad (7)$$

$$J_{ITAE} = \int_0^{t_{max}} t * abs(T_{out} - T_{ref}) dt \quad (8)$$

The optimization was performed with the mode FRONTIER optimization software (see Fig. 8), using the MOGA-II algorithm (130 generations and a probability of directional cross-over equal to 0,5), coupled with the Matlab/Simulink accumulator model.

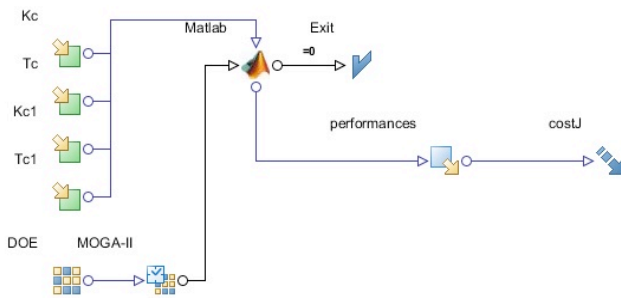


Fig. 8. Optimization scheme in mode FRONTIER

#### Controllers switching strategy optimization

The switching strategy function between each controller is optimized together with the controllers themselves. The chosen cost function is the ITEA criteria given in the previous part. Different mathematical interpolation laws can be applied between the two controllers. In this paper we tried to optimize controllers for four types of controller interpolation strategies given below. An optimal controller is found for each controller interpolation strategy.

The first one is a linear interpolation:

$$\beta_1 = \frac{V_{inaccu}}{V_0} \quad (9)$$

with  $V_{inaccu}$  the accumulator input velocity and  $V_0$  the nominal accumulator velocity.

The second one is a parabolic interpolation:

$$\beta_2 = \frac{V_{inaccu}^2}{V_0^2} \quad (10)$$

The third one is an interpolation represented by a sigmoid function, the fourth interpolation method  $\beta_4$  is a custom function.

$$\beta_3 = \left( \frac{1}{1 + \exp^{-5 \cdot V_{inaccu}}} - 0.5 \right) * 2 \quad (11)$$

#### Mono-objective robust controllers optimization

As shown in part 2.2, the accumulator dynamic performances depend on the web elasticity. Consequently, our goal is to find the most robust controllers for a large of Young modulus variation. In order to obtain this robustness, the cost function has to take into account Young modulus changes. The cost function  $J_{ROB}$ , given in relation (12), is composed of the sum of the ITAE criterion calculated for each Young modulus value in the simulated accumulator. The selected interpolation strategy is  $\beta_3$ .

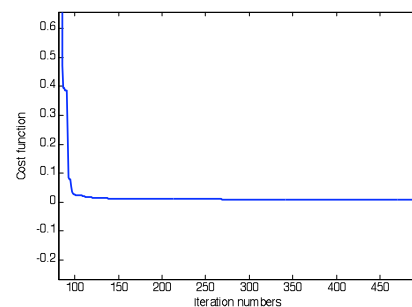
$$J_{ROB} = \sum_{E_{min}}^{E_{max}} \int_0^{t_{max}} t * abs(T_{out_E} - T_{ref}) dt \quad (12)$$

In this study three Young modulus values were used:  $E_0$ ,  $E_0$  multiplied by 5 and  $E_0$  divided by 5.

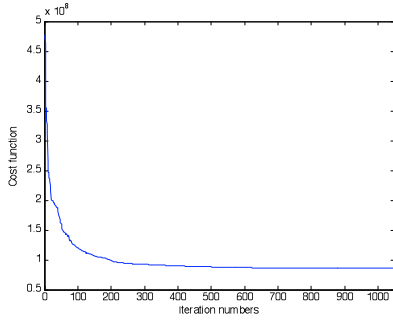
### 3.3 Optimization results

#### Mono-objective controllers optimization results

The evolution of the cost function  $J$  is shown on Fig. 9(a) and the evolution of the cost function  $J_{ITAE}$  is given in Fig. 9(b). The data have been sorted from the highest to the lowest value of each cost function. In reality, cost functions have more dissemination due to the use of a genetic algorithm. Fig. 10 shows the evolution of the controller  $C_1$  parameters corresponding to cost function  $J$ . Fig. 11 gives the evolution of the controller  $C_1$  parameters corresponding to cost function  $J_{ITAE}$ .

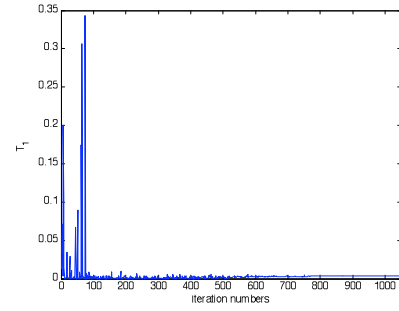


(a) Cost function  $J$



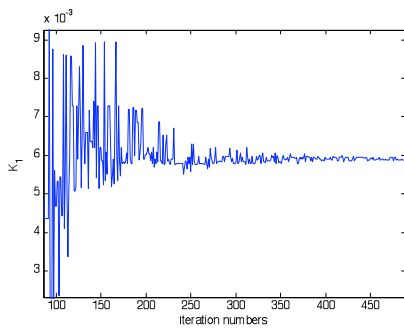
(b) Cost function  $J_{ITAE}$

Fig. 9. Evolution of the cost function  $J$  and  $J_{ITAE}$

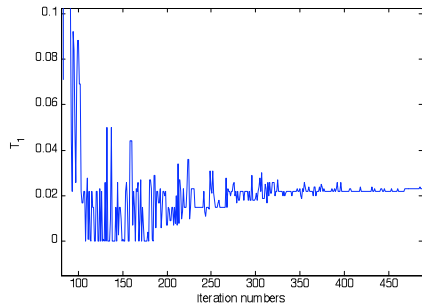


(b) Integral gain  $\tau_1$

Fig. 11. Controller  $C_1$  parameters for criterion  $J_{ITAE}$



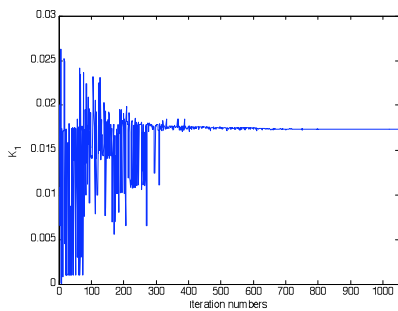
(a) Proportional gain  $K_1$



(b) Integral gain  $\tau_1$

Fig.10. Controller  $C_1$  parameters for criterion  $J$

As observed on Fig. 10,  $C_1$  parameters using cost function  $J$  converge rapidly to an optimal value.



(a)Proportional gain  $K_1$

Using cost junction  $J_{ITAE}$  does not really change the rapidity of the genetic algorithm convergence. But as seen on Fig. 11,  $J_{ITAE}$  leads to other controller values, as expected. This highlights that it's very important to adequately chose the cost function. The control strategy has also been optimized with the other switching strategies  $\beta_2$ ,  $\beta_3$  and  $\beta_4$ .

In this part, the controllers and switching strategies were optimized together.

A second optimization strategy consists to optimize sequentially the controllers. The simulation results are given in the part 3.4.

**Robust controllers with mono-objective optimization**

As observed on Fig. 12, the cost function  $J_{ROB}$  converges rapidly to an optimal value which is higher than  $J_{ITAE}$ . The algorithm has to find the best controllers for all the range of Young modulus, and therefore it is more robust but less performing. Nevertheless, the optimization algorithm needs more time for this controller synthesis strategy.

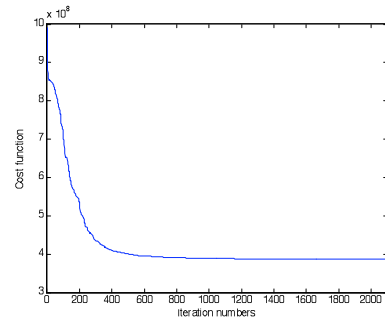


Fig.12. Evolution of the cost function  $J_{ROB}$

**3.4 Simulation results**

**Mono-objective controllers optimization simulation results**

One can observe on Fig. 13 that optimized PI controllers leads to better tension regulation performances as hand tuned controllers. During a wound roll change phase which is the more critical production step (section d, e and f on Fig. 13), optimized controllers significantly reduce tensions variations while the input velocity is dropping to zero.

As expected, optimizing controllers together leads to better performances than sequentially optimizing. During the charging phase (section b), during the maximum web length phase (section c) and during the wound roll change phase, PI controllers optimized together gives the best results and reduce significantly web tensions variations.

**Accumulator simulation sequence**

- a: The accumulator is at its nominal web length, velocity and tension.
- b: The accumulator carriage is moved up to reach the maximum web length; the velocity is increased to maintain nominal web tension.
- c: The accumulator is charged and maintained at maximum web length.
- d: The input velocity decreases and the accumulator carriage is moved down to release web and maintain the nominal web tension.
- e: The input velocity is equal to zero, the accumulator carriage is moved down to restore web and maintain the nominal web tension.
- f: The input velocity increases to reach the nominal velocity, the accumulator carriage is moved down to restore web and maintain the nominal web tension.
- g: The accumulator is maintained at a constant position to maintain a constant web length, web velocity and web tension in the accumulator.

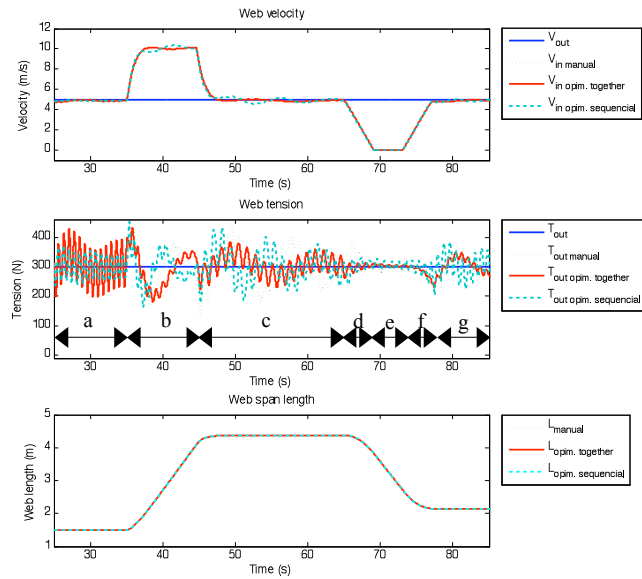


Fig. 13. Optimized PI controllers simulation results using cost function  $J$  for switching strategy  $\beta_1$

**Controllers switching strategy optimization simulation results**

As we can see on Fig. 14, using controllers interpolation strategies  $\beta_1, \beta_2$  or  $\beta_3$  leads to similar performances because controllers are optimized together with the switching function. Only the custom strategy  $\beta_4$  seems to give better performances.

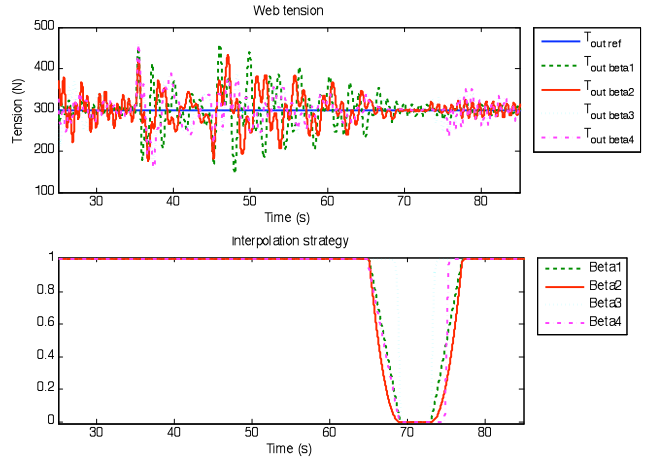


Fig. 14. Optimized PI controllers simulation results using cost function  $J_{ITAE}$  for different switching strategies

**Simulation of robust controllers with mono-objective optimization**

Fig. 15 to 17 show the simulation results for three different Young modulus values. The obtained performances are maintained in acceptable range from  $E_0$  divided by 5 to  $E_0$  multiplied by 5, using  $J_{ROB}$  as cost function. Nevertheless, if we consider only the nominal point  $E_0$ , the performances are better for the controller optimized for  $E_0$  alone (cost function  $J_{ITAE}$ ). This implies that we have to make a compromise between performances and robustness to web elasticity variations. Therefore a multi-objective optimization approach will be studied in the next future.

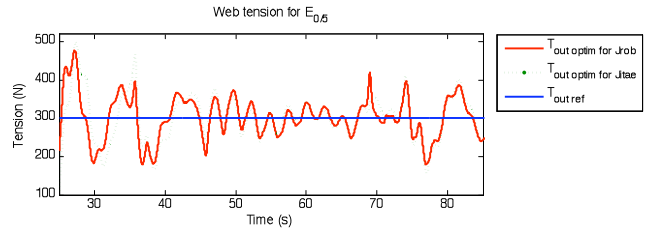


Fig. 15. Optimized PI controllers simulation results for  $J_{ROB}$  or  $J_{ITAE}$  using switching strategy  $\beta_2$  (for  $E_0/5$ )

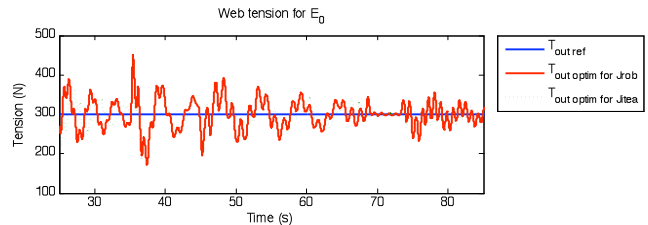


Fig. 16. Optimized PI controllers simulation results for  $J_{ROB}$  or  $J_{ITAE}$  using switching strategy  $\beta_3$  (for  $E_0$ )

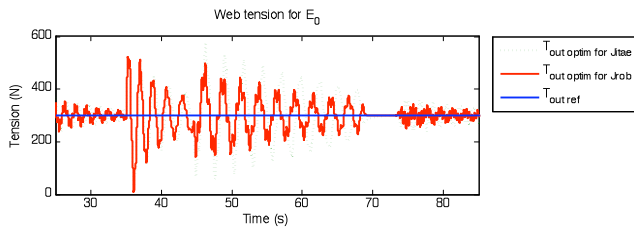


Fig. 17. Optimized PI controllers simulation results for  $J_{ROB}$  or  $J_{ITAE}$  using switching strategy  $\beta_3$  (for  $5 \cdot E_0$ )

## 4 Conclusions

This study presents first the physical equations used in the modeling of an industrial accumulator. The nonlinear model, programmed in Matlab/Simulink software environment, enables a model based optimization of the controllers together with the controllers switching strategy. Several mono-objective controller optimization strategies are presented and simulation results are compared. Improved dynamic behaviours have been obtained using optimized controllers, in comparison to hand tuned controllers. Nevertheless, a compromise between web tension control performances and robustness against web elasticity variations has to be made. Therefore applying a multi-objective optimization approach will be the next step of our work.

## Acknowledgement

The authors wish to thank Region Alsace for having partly funded this research and the Monomatic France company for their very helpful discussions.

## References

1. A. Benlatreche, D.Knittel, and E.Ostertag, "Robust decentralized control strategies for large-scale web handling systems", *Control Engineering Practice*, vol.16, 736-750(2008)
2. G. Brandenburg, "Über das dynamische Verhalten durchlaufender elastischer Stoffbahnen bei Kraftübertragung durch Coulomb'sche Reibung in einem System angetriebener, umschlungener Walzen", Doctoral Thesis, Technischen Universität München (1971)
3. J. Frechard, D. Knittel, P. Dessagne, J.S. Pellé, G. Gaudiot, J.C. Caspar, G.Heitz, "Modelling and fast position control of a new unwinding-winding mechanism design", *Electrimacs 2011*, Cergy-Pontoise, France (2011)
4. V.Gassmann, D.Knittel, P.R.Pagilla, M.-A.Bueno, "H $\infty$  unwinding web tension control of a strip processing plant using a pendulum dancer" *American Control Conference, ACC '09.*, 901-906(10-12 June 2009)
5. V. Gassmann, D. Knittel, J. Frechard, "Multi-Objective Robust Controller Optimization for Complex Mechatronic Systems Design: Application to Roll-to-Roll Systems", 12<sup>e</sup> congrès annuel de la Société Française de Recherche Opérationnelle et d'Aide à la Décision, ROADEF 2011, St Etienne, France, 2011.
6. D. Knittel, A. Arbogast, M. Vedrine, and P.R. Pagilla, "Decentralized robust control strategies with model based feed forward for elastic web winding systems", in *American Control Conference*, Minneapolis, Minnesota, USA (2006)
7. D. Knittel, L. Federlin, M. Boutaous, P. Bourgin, M. Loesh, and B. Muller, "Modelling and tension control of an industrial winder with dancer mechanism", in *IFAC Symposium on Automation in Mining, Mineral and Metal processing, MMM'2004*, Nancy, France (2004)
8. D. Knittel, E. Laroche, D. Gigan, and H. Koc, "Tension control for winding systems with two-degrees-of-freedom H $\infty$  controllers", *IEEE Transactions on Industrial Applications*, vol. 39, 113-120 (2003)
9. H. Koc, "Modélisation et commande robuste d'un système d'entraînement de bande flexible" PhD Thesis, Louis Pasteur University, Strasbourg, France (2000)
10. H. Koc, D. Knittel, M. De Mathelin, and G. Abba, "Modeling and robust control of winding systems for elastic webs", *IEEE Transactions on Control Systems Technology*, vol. 10, 197-206 (2002)
11. H. Koç, D. Knittel, M. de Mathelin, G. Abba, C. Gauthier, "Web tension control in an industrial accumulator", *Proceeding of the 5<sup>th</sup> International Conference on Web Handling, IWEB5*, Stillwater (Oklahoma), USA (1999)
12. H. Koç, D. Knittel, G. Abba, M. de Mathelin, C. Gauthier, E. Ostertag, "Modeling and control of an industrial accumulator in a web transport system", *Proceeding of the European Control Conference ECC'99* (Sept. 1999)
13. D. Kuhm, D. Knittel, M-A. Bueno, "Modelling and robust control of an industrial accumulator in roll to roll systems", *Proceeding of the 35<sup>th</sup> Annual Conference of the IEEE Industrial Electronics Society, IECON09*, Porto, Portugal (2009)
14. D. Kuhm, D. Knittel, "New design of robust industrial accumulators for elastic webs", 18<sup>th</sup> World Congress of the International Federation of Automatic Control, IFAC, Milano, Italy (2011)
15. D. Knittel, D. Kuhm, "Multidisciplinary design optimization of an accumulator for a large elasticity range of flexible webs", *Proceeding of the Third International Conference on Multidisciplinary Design Optimization and Applications*, 21-23 June 2010, Paris, France
16. D. Knittel, J. Frechard, M. Vedrines, "Multi-objective optimization for manufacturing process design: application in roll-to-roll systems", *Proceeding of the Third International Conference on Multidisciplinary Design Optimization and Applications*, 21-23 June 2010, Paris, France
17. C. L. Lin, H. Y. Jan, "Multi objective PID control for a linear brushless DC motor: an evolutionary approach", *IEE Proceedings -Electric Power Applications*, vol. 149, No 6(Nov 2002)
18. V. Gassmann, "Commande décentralisée robuste de systèmes d'entraînement de bandes à élasticité variable", PhD Thesis, University of Strasbourg, Strasbourg, France (2011)
19. P.R. Pagilla, S.S. Garimella, L.H. Dreinhoefer, E.O. King, "Dynamics and Control of Accumulators in Continuous Strip Processing Lines", *IEEE Transactions On Industry Applications*, Vol. 37, No. 3 (May/June 2001)
20. P.R. Pagilla, I. Singh, R.V. Dwivedula, "A study on control of accumulators in web processing lines", *Proceeding of the American Control Conference* (2003)
21. A. Popov, A. Farag, H. Werner, "Tuning of a PID controller using a multi-objective optimization technique applied to a neutralization plant", *European Control Conference 2005*, Seville, Spain(2005)

22. W. Wolfermann, *"Tension control of webs - a review of the problems and solutions in the present and future"* Proceeding of the 3<sup>rd</sup>International Conference on Web Handling, IWEB3, Oklahoma, 198-229 (1995)
23. N. Zahlan, and D.P.Jones, *"Modeling web traction on rolls"*, Proceeding of the 3<sup>rd</sup>International Conference on Web Handling, IWEB3, Oklahoma, 156-171 (1995)
24. K. Zielinski, M. Joost, R. Laur, B. Orlik, *"Comparison of differential evolution and particle swarm optimisation for the optimisation of a PI cascade control"*, IEEE Congress on Evolutionary Computation (2008)